Aalborg Universitet

Using guaiacol as a capping agent in the hydrothermal depolymerisation of kraft lignin

Ahlbom, Anders; Maschietti, Marco; Nielsen, Rudi; Hasani, Merima; Theliander, Hans

Link to publication from Aalborg University

DE GRUYTER

Nord. Pulp Paper Res. J. 2023; 38(4): 619–631

Lignin

Anders Ahlbom, Marco Maschietti, Rudi Nielsen, Merima Hasani* and Hans Theliander

Using guaiacol as a capping agent in the hydrothermal depolymerisation of kraft lignin

Abstract: The depolymerisation of softwood kraft lignin was investigated, under hydrothermal conditions at 290 °C and 250 bar, with guaiacol in the reactor feed to evaluate its impact on the formation of char and on the molecular weights of the products. The effect of residence time was investigated in the time span 1–12 min. Lignin is depolymerised during the process and guaiacol is both formed and consumed during the reaction, with clearly noticeable changes as early as in the first minute of reaction. Although the addition of guaiacol in the reactor feed causes a reduction in the weight average molecular weight of the products, the yield of char increases. Longer residence times result in repolymerisation of the reaction products as well as a further increase in the yield of monoaromatic components and char.

Keywords: capping agent; guaiacol; HTL; hydrothermal depolymerisation; kraft lignin

1 Introduction

Lignin, the polymer in lignocellulosic biomass formed of aromatic phenylpropane units, has a good potential of becoming a source of renewable aromatic molecules (Balakshin et al. 2021). Most of the lignin processed industrially is kraft lignin, from the kraft pulping process which liberates lignin from wood. In this process, the lignin structure changes as inter-unit linkages are cleaved and condensation reactions occur. Furthermore, aromatic rings are cleaved from aliphatic side chains with retro-aldol reactions, leaving a lignin structure

different from the native lignin (Crestini et al. 2017; Giummarella et al. 2020). The content of aromatic rings and the large scale of kraft lignin production, coupled with techniques of isolation of lignin from the black liquor, e.g. the LignoBoost process, attracts attention to kraft lignin. In order to facilitate the use of the aromatic functionalities, the lignin macromolecule can be depolymerised. Aromatics can thereby be accessed for use as e.g. chemicals or producing resins (Dessbesell et al. 2020; Goldmann et al. 2020). Several ways of depolymerising lignin have been investigated, including pyrolysis, oxidative methods, hydrothermal methods and hydrogenolysis (Cao et al. 2020; Galkin and Samec 2016; Kleinert and Barth 2008). Hydrothermal methods are of particular interest since they employ water, which is a non-toxic reaction medium and a reactant that, at high temperature and pressure, opens hydrolytic reaction pathways (Brand et al. 2014). Moreover, hydrothermal methods do not require drying of the starting material. The ionic product and the dielectric constant change as the water temperature approaches the critical point, enabling the dissolution of less polar components and providing a high concentration of H_3O^+ and OH^- ions, which favour hydrolysis reactions (Lappalainen et al. 2020). Hydrolysis of lignin is also promoted in alkaline reaction conditions (Toor et al. 2011). Applying hydrothermal methods at different temperatures gives different major products (Kruse and Dahmen 2015). Carbonisation, which predominately yields solid products, occurs at low reaction temperatures (180–250 °C) whilst liquefaction, used to produce bio-oil or bio-crude, occurs at intermediate temperatures (250–400 °C) and gasification occurs at even higher temperatures (>400 °C) (Brand et al. 2014).

Depolymerisation of lignin is accompanied by repolymerisation reactions of the products (Islam et al. 2018; Jensen et al. 2017). Char is formed as the reaction products repolymerise in the reaction mixture, which poses problems with the loss of valuable low molecular weight material to a high molecular weight fraction with limited value, except as fuel (Toledano et al. 2014). Char can also cause operational problems by blocking valves and tubes in the reactor system (Belkheiri et al. 2014). It has been proposed that the formation of char can be mitigated by the use of capping agents,

*Corresponding author: Merima Hasani, Dept. of Chemistry and Chemical Engineering, Chalmers University of Technology, SE-412 96 Gothenburg, Sweden, E-mail: merima.hasani@chalmers.se
Anders Ahlbom and Hans Theliander, Dept. of Chemistry and Chemical Engineering, Chalmers University of Technology, SE-412 96 Gothenburg, Sweden. https://orcid.org/0000-0002-5055-041X (A. Ahlbom)
Marco Maschietti and Rudi Nielsen, Dept. of Chemistry and Bioscience, Aalborg University, Niels Bohrs Vej 8, DK-6700 Esbjerg, Denmark

which are chemicals added to the reaction mixture to scavenge reactive lignin derivatives. While aliphatic alcohols (Ahlbom et al. 2021; Cheng et al. 2012; Guo et al. 2021; Lee et al. 2016), boric acid (Roberts et al. 2011; Toledano et al. 2014) and phenol (Arturi et al. 2017; Belkheiri et al. 2018; Nguyen et al. 2014; Toledano et al. 2014) have all been investigated as capping agents, it has also been suggested that phenols liberated from the lignin structure itself can be recirculated to the reactor to act as capping agents (Belkheiri et al. 2018; Hernández-Ramos et al. 2020; Okuda et al. 2004).

When softwood lignin is being depolymerised, one of the most common phenolic reaction products is guaiacol, which is probably due to softwood lignin being built mainly of guaiacyl propane units (Abdelaziz et al. 2018; Gellerstedt 2015). Guaiacol could therefore be available for recirculation as a capping agent in a continuous reactor. As far as the authors are aware, the effect of guaiacol when used as a capping agent in the depolymerisation of kraft lignin with respect to char yield and molecular weights of the products, has not been investigated as yet; the aim of work is to contribute to filling this gap in knowledge.

2 Materials and methods

2.1 Materials

Softwood kraft lignin isolated from black liquor by the LignoBoost process at the Bäckhammar Mill in Sweden from *Pinus sylvestris* and *Picea abies*, with a dry content of 82.9 % ± 1.2 % (Sartorius MA30 moisture analyser; Sartorius, Göttingen, Germany) and a sulphur content of 1.97 wt% ± 0.2 wt% (Ahlbom et al. 2021), was depolymerised in a mixture of guaiacol (≥99 %, Sigma-Aldrich, Steinheim, Germany), anhydrous sodium carbonate (≥99.9 %, VWR Chemicals, Leuven, Belgium), sodium hydroxide (≥99 %, Merck, Darmstadt, Germany) and deionised water.

The following were all used as received for the analytical measurements: LiBr (>99 %, Sigma-Aldrich, Steinheim, Germany), dimethyl sulphoxide (DMSO, >99.7 %, Sigma-Aldrich, Steinheim, Germany), pullulan standards (PL2090-0100, Varian, Church Stretton, UK), sodium standard (UltraScientific, North Kingstown, USA), diethyl ether (DEE, >99.0 % with 1 ppm BHT as the inhibitor, Sigma-Aldrich, Steinheim, Germany), nitric acid (65 %, Merck Suprapur, Darmstadt, Germany), syringol (99 %, Sigma-Aldrich, Steinheim, Germany), DMSO-d_6 (99.5 atom% D, 0.03 (v/v) TMS, Sigma-Aldrich, Sigma-Aldrich, Steinheim, Germany), 1,2-dihydroxybenzene (>99 %, Sigma-Aldrich, Steinheim, Germany), guaiacol (Sigma-Aldrich, Steinheim, Germany), 1,2-dimethoxybenzene (99 %, Sigma-Aldrich, Steinheim, Germany), 4-methyl guaiacol (≥98 %, Sigma-Aldrich, Steinheim, Germany), 4-ethylguaiacol (≥98 %, Sigma-Aldrich, Steinheim, Germany), vanillin (99 % Sigma-Aldrich, Steinheim, Germany), acetovanillone (≥98 %, Sigma-Aldrich, Steinheim, Germany), homovanillic acid (Sigma-Aldrich, Steinheim, Germany) and HCl (1 M, Honeywell Fluka, Seelze, Germany).

2.2 Methods

Softwood kraft lignin was depolymerised at a mass fraction of 5 wt% in a mixture of water, sodium carbonate (1.6 wt%), sodium hydroxide

(1.0 wt%) and guaiacol (0–2 wt%). The reactor employed was a custom-made 99 ml batch reactor that allows a charge (containing lignin, base, water and guaiacol mixed for 15 min at 15,000 rpm with an Ultra-Thurrax [IKA T25; IKA-Werke GmbH & Co. KG., Staufen, Germany]) to be injected into a preheated pre-charge. Non-reactive species in the precharge, such as water and salts, can thereby be heated to a temperature greater than that of the reaction. The injection is thus made into a mixture of vapour and liquid, where the condensation of the vapour heats the injection charge. The reaction charge quickly reaches the reaction temperature desired which, together with a rapid cooling down after the reaction, is beneficial to the hydrothermal treatment of biomass (Brand et al. 2014). A more in-depth description of the reactor is given by Arturi et al. (2017).

The injection causes the temperature in the reactor to fall, after which the control system of the reactor aims at re-establishing the set point temperature; this is also accompanied by small variations in pressure but these can be controlled by minor injections and ejections (<1 ml) of reaction material. In this work, the residence time of the reaction mixture was defined as the time between the end of the injection and the start of the discharge. Since the temperature and pressure vary during the residence time, an average reaction temperature and an average reaction pressure were defined as

$$y_{\mathrm{avg}} = \int_{t_1}^{t_2} y(t)\, dt \big/ (t_2 - t_1) \tag{1}$$

where y is either pressure or temperature, and t_1 and t_2 are the times of the end of the injection and the start of the discharge, respectively.

At the end of the residence time in the reactor, the product was discharged into a flask containing 200 g water placed in an ice-bath to quench the reacting mixture and halt the reactions. No quantification, nor identification, of gases formed was made. A sample was taken to measure the guaiacol content in the product fraction by gas chromatography using a flame ionisation detector (GC-FID). The product was then fractioned into three parts: char, precipitated solids (PS) and acid soluble organics (ASO). This fractionation is outlined in Figure 1, along with the analytical procedures. The reactor product was divided in two product fractions and each was filtered over a #5 glass filter, with a nominal cut-off of 1.0–1.6 μm. The resulting filter cake was washed with a water amount equivalent to half the filtered product liquor to remove residual product liquor containing guaiacol, and was dried at 40 °C for four days to give the *char* fraction. Data presented of the char yield is reported as the average and standard deviation of the two filtrations.

The filtrate was acidified with 1 M HCl to pH 1.5 to precipitate the solids, which were filtered over a #5 glass filter. The resulting filter cake was washed with an equal amount of water as the acid filtrate sample, again to dispel potential residual guaiacol. The filter cake was then dried at 40 °C for five days, thereby forming the *PS* fraction.

The remaining acid filtrate was dried at ambient conditions for three days, followed by drying at 40 °C for a day, to give the *ASO* fraction. It is assumed that residual guaiacol from the reaction mixture will be found in this ASO phase because guaiacol is soluble in the reaction mixture. Salt crystals, most likely NaCl resulting from acidification of the Na_2CO_3 and NaOH with HCl, were found in the ASO fraction as the water was being evaporated. In order to quantify this amount of NaCl, the sodium content of the acidified filtrate was measured by inductively-coupled plasma – optical emission spectrometry (ICP-OES) and, assuming all of the sodium was present as NaCl, this content of salt was deducted from the ASO yield.

Yields of char, PS, ASO and monoaromatic compounds were calculated based on the dry lignin loaded to the reactor accordingly:
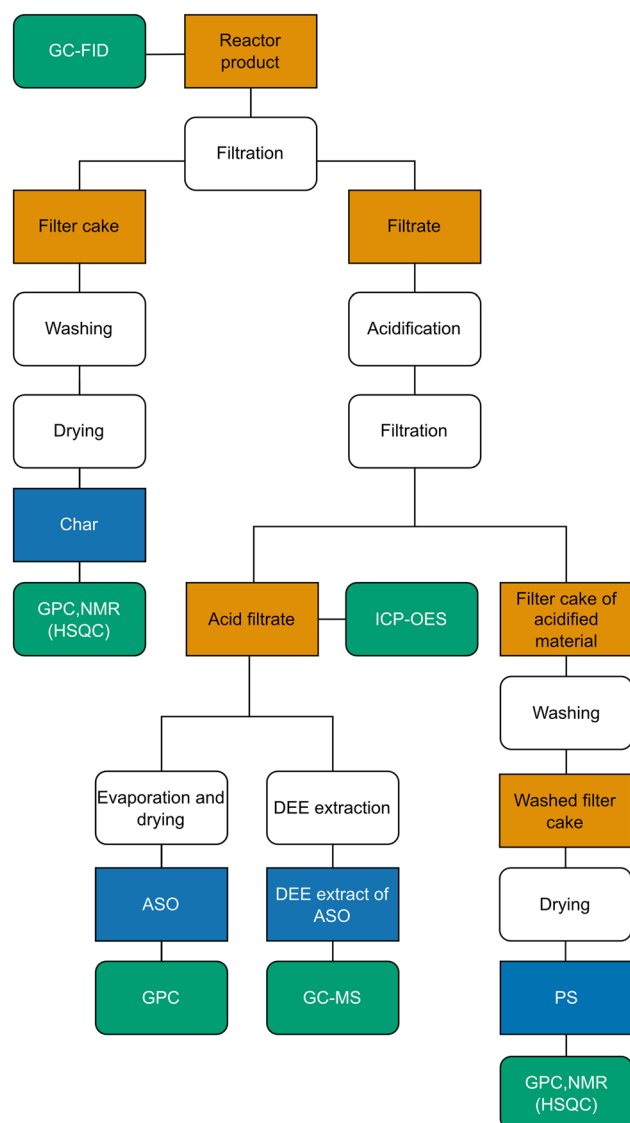
Figure 1: Fractionation flow chart of the reactor product.

$$Y_i = 100 \times \frac{m_i}{m_{\mathrm{dry\,lig}}} \tag{2}$$

with Y_i being the yield of fraction i, m_i the mass of fraction i and $m_{\mathrm{dry\,lig}}$ the mass of dry weight lignin loaded to the reactor.

2.3 Analytical procedures

2.3.1 GC-FID: The guaiacol present in the product mixture was measured by a gas chromatograph equipped with a flame ionisation detector (GC-FID; PerkinElmer Clarus 690; PerkinElmer Inc., Waltham, Massachusetts, USA). 1 ml product phase was acidified with 0.3 ml 2 M HCl to pH 0–1. Then, 1 ml of the acidified product phase was mixed with 1 ml internal standard solution (4 g/l phenol in water), filtered using a 0.45 μm syringe filter and run in GC-FID. The phenol formed in the reaction constituted <0.1 % of the phenol in the sample injected, enabling phenol to be used use as an internal standard. The column was an *Elite BAC-1 Advantage* that was 30 m long, with an internal

diameter of 0.32 mm and a film thickness of 1.8 μm. The injection temperature was 250 °C with a 1:50 split ratio; the temperature programme was 120 °C which was held for 1 min, followed by heating at the rate of 30 °C/min to 225 °C, at which the temperature was held for 1.5 min. Duplicate samples were run with double injections; the average relative standard deviation was found to be 2.5 %.

2.3.2 GC-MS: Gas chromatography mass spectrometry (GC-MS; Agilent 7890A; Agilent Technologies Co. Ltd., Shanghai, China and Agilent 5975C; Agilent Technologies Inc., Wilmington, DE, USA) was used for identification and semi-quantification of molecules of low-molecular weight in the product. 5 ml of the acidified product filtrate was added to 0.5 ml internal standard (1 g/l syringol in water) and extracted 1:1 w/w with DEE. The samples were filtered on 0.45 μm filters, injected with a split ratio of 1:19 and an inlet temperature of 300 °C and then run with a helium flow of 1 ml/min through an *HP-5MS UI* (Agilent Technologies Inc., Santa Clara, CA, USA) column. The temperature of the column started at 70 °C for 2 min, followed by heating at a rate of 20 °C/min to 275 °C, at which the temperature was held for 10 min. The MS Quad was run at 150 °C and the MS Source at 230 °C. Compounds were identified using the programme NIST MS Search 2.2, employing the library NIST11. This identification was subsequently confirmed by matching the retention times with pure components. Semi-quantification of the components was made using the relation

$$W_i = W_{IST}A_i/A_{IST}, \tag{3}$$

where A is the peak area in the chromatogram, W the mass fraction in the sample, i the analyte in the samples and *IST* the internal standard (Nguyen et al. 2014). Samples were analysed in duplicate; the average relative standard deviation was found to be 5.0 %.

2.3.3 GPC: Molecular weight distributions were measured by gel permeation chromatography (GPC, PL-GPC 50 Plus Integrated GPC system, Polymer Laboratories; Varian Inc., Church Stretton, UK). Samples were prepared at 0.24 g/l concentration (3 g/l in the case of testing a control sample of non-reacted guaiacol without lignin) in the eluent, DMSO with 10 mM LiBr added. Samples were filtered through 0.2 μm GHP syringe filters. Two PolarGel-M columns (300 × 7.5 mm) and a pre-column (PolarGel-M, 50 × 7.5 mm) were employed, the temperature was set at 50 °C and the eluent flow rate was 0.5 ml/min. An ultra-violet light (UV) detector, operating at 280 nm, was used and calibration was made with pullulan standards. Double injections of samples were run, and the average relative standard deviation was 0.92 %. Data processing was made with Cirrus GPC Software 3.2.

2.3.4 NMR (HSQC): Nuclear magnetic resonance spectroscopy (NMR) was utilised to investigate changes in the molecular structure of the char and PS fractions. Heteronuclear single quantum coherence (HSQC) spectra were recorded at 25 °C on an 800 MHz spectrometer, with a 5 mm TXO cold probe (Bruker Avance II HD; Bruker BioSpin GmBH, Rheinstetten, Germany) at 25 °C. The pulse programme *hsqcedetgpsisp2.3* was used, with an acquisition time of 96 ms for ^{1}H and 6 ms for ^{13}C. The spectra were recorded in an edited mode, with 1 s relaxation delay and 24 scans. A total of 3072 and 512 points were acquired for the ^{1}H and ^{13}C dimensions, respectively. Samples were dissolved overnight, to a concentration of 140 g/l in DMSO-d_6. They were then centrifuged at 12,045×g for 5 min before the supernatant was transferred to 3 mm tubes and run in the spectrometer.

The NMR spectra were divided into three regions: aliphatic, inter-unit and aromatic, according to the method presented by Mattsson et al. (2016). Ether linkages, such as β-O-4′ and ether portions of the C–C bonds, β-β′ and β-5′, appear in the inter-unit region.

2.3.5 ICP-OES: The sodium content of the ASO fraction was measured by inductively-coupled plasma – optical emission spectrometry (ICP-OES; Thermo Scientific iCAP Pro, Thermo Fischer, Cambridge, UK). The filtrate of the acid product was filtered using 0.45 μm syringe filters and then diluted 1:50 with 0.5 M HNO_3 containing an internal standard of 2 ppm yttrium. The intensity of the sodium emission line at 589.59 nm was measured in triplicate for each sample, with an average relative standard deviation of 6.1 %.

2.4 Test plan

The test plan included 10 experimental runs, with residence times in the range 1–12 min, for four nominal levels of guaiacol mass fractions in the range 0–2 wt%, see Table 1. The injection of the charge containing the lignin and guaiacol aimed to reach a pressure in the reactor of 250 bar after heating to the reaction temperature. The resulting mass fraction of lignin was in the range 5.1–5.4 wt%, while the mass fractions of guaiacol at the four levels were 0, 0.2, 1.1 and 2.1–2.2 wt%, as reported in the table. A control sample without lignin was run to investigate the stability of guaiacol under the reaction conditions.

It was estimated from the experimental data of a previous work (Ahlbom et al. 2022) that the mass fraction of guaiacol in the product mixture could be around 0.2 wt%. This was chosen as the lowest mass fraction level to evaluate the effect of the capping agent as opposed to no guaiacol loading. Furthermore, previous work (Belkheiri et al. 2018) also showed that increasing the mass fraction above 2 wt% of the capping agent, in that case phenol, did not improve the yield of either bio-oil or water-soluble organics significantly. Consequently, the highest mass fraction of guaiacol added in this study was chosen as 2 wt%. Moreover, 2 wt% guaiacol in the feed was also close to the limit of mass fraction of guaiacol in the injection charge at which it was possible to mix and pump the charge in the injection system: at higher mass fractions, the separation of a highly viscous guaiacol-rich phase was observed.

There are two duplicate sets of experiments, with a nominal mass fraction of 0 and 2 wt% guaiacol in the reactor feed, respectively, at 4 min residence time. The yield data and content of guaiacol after the reaction are presented as averages of the two experiments, along with their standard deviations.

3 Results

The product formed after hydrothermal treatment and quenching in the cold trap was an aqueous liquid with a smoky odour. The product fractionation resulted in three fractions: char, PS and ASO. However, not all conditions yielded char: no char was formed at 1 min of residence time when the reaction mixture did not contain guaiacol. Nor did char appear in the control sample containing guaiacol run without lignin. Furthermore, in the control sample, only a very small amount of PS was formed: too little to be quantified accurately. This suggests that char and PS indeed originate from the lignin added to the system, and not from the guaiacol added.

3.1 Reactions of guaiacol

In Figure S1, the content of guaiacol remaining in the product is presented as fractions of the mass fraction of guaiacol in the reactor feed. The control experiment, without lignin but with guaiacol, was performed in order to investigate the reactions of the guaiacol. Neither char nor PS were then formed, but Figure S1 shows that about 45 % of the guaiacol in the feed was consumed in the control experiment, thereby confirming that guaiacol reacts during the treatment. The products of the guaiacol reaction, however, remain dissolved both before and after acidification to pH 1.5 and end up in the ASO fraction. The oxygen content of guaiacol could possibly result in the products of the reacted guaiacol

Table 1: Test plan for the study, including the resulting T_{avg}, P_{avg} and pH of the product. T_{avg} and P_{avg} refer to average temperatures and pressures during the sample residence in the reactor.

Nominal guaiacol in the feed [wt%]	Residence time [min]	Na$_2$CO$_3$ [wt%]	NaOH [wt%]	Water [wt%]	Guaiacol [wt%]	Lignin [wt%]	T_{avg} [C]	P_{avg} [bar]	pH of product
2	4	1.6	1.0	95.2	2.2	0.0	294	243	12.4
0	1	1.6	1.0	92.2	0.0	5.2	291	214	10.9
2	1	1.6	1.0	90.0	2.1	5.3	291	249	10.3
0	4	1.6	1.0	91.9	0.0	5.5	288	247	10.5
0	4	1.6	1.0	92.1	0.0	5.3	294	214	10.1
0.2	4	1.6	1.0	92.1	0.2	5.1	293	248	10.5
1	4	1.6	1.0	91.0	1.1	5.3	295	249	10.1
2	4	1.6	1.0	89.9	2.2	5.4	301	251	10.0
2	4	1.6	1.0	90.2	2.1	5.2	296	241	10.2
2	12	1.6	1.0	89.8	2.2	5.4	295	248	10.1

having oxygen-containing functional groups that cause it to remain dissolved, or be present in some colloidal form, thus avoiding precipitation in the aqueous product phase.

The molecular weight distribution of the ASO fraction of the control experiment is shown in Figure S2, together with samples run at the same reaction conditions but also including lignin. As can be seen, the ASO fraction without lignin shows components of high molecular weight. Indeed, oligomeric and polymeric fractions are formed. These fractions show a weight average molecular weight (M_w) of 8.0 kDa, see Table S1, which indicates a degree of polymerisation of guaiacol of about 65. Polymerisation of guaiacol has been reported previously in supercritical water and in pyrolysis; in these cases, the polymerised guaiacol formed a precipitating char fraction (Lawson and Klein 1985; Wahyudiono et al. 2011, 2007). However, at sub-critical conditions, 250 °C, no char was formed but crosslinking of guaiacol derived phenolic structures from was noted (Wahyudiono et al. 2011).

An investigation into the behaviour of guaiacol at high pH at ambient temperature was also carried out to verify whether high pH alone causes polymerisation. No formation of high M_w products occurred, though the mixture turned from clear via blue to dark brown in 2 h, similar to the observations of Taurog et al. (1992). It was thus confirmed that polymerisation of guaiacol did not occur spontaneously in the reaction mixture but required elevated temperatures and pressures.

Identification of monoaromatic compounds with GC-MS in the product mixture of the control experiment, with guaiacol but without lignin added, showed that guaiacol, aside from polymerising, also formed 1,2-dimethoxybenzene. At higher temperatures, and without any alkaline components added, guaiacol was instead reported to form catechol, phenol, o-cresol and methanol (Lawson and Klein 1985; Wahyudiono et al. 2011, 2007).

The reactions of guaiacol, with lignin in the reaction mixture, are presented in the following sections. Figure 2 shows the mass of guaiacol in the product mixtures at varying residence times (A) and additions of guaiacol (B). From the experiments without any guaiacol in the feed, it can be seen that the formation of guaiacol starts within the first minute of reaction, and that the net rate of formation slows down between 1 and 4 min, see Figure 2A. Furthermore, when starting with 2 wt% guaiacol in the feed, the rate of consumption of guaiacol is higher in the first minute and decreases as the reaction time increases, see Figure 2A. Formation of guaiacol from lignin could include retro-aldol reactions cleaving of side chains from the guaiacyl unit similar to reactions during kraft pulping (Crestini et al. 2017; Giummarella et al. 2020). Guaiacol is therefore both formed

and consumed during hydrothermal treatment. In the absence of guaiacol in the feed, there is a net production of guaiacol from lignin depolymerisation whereas, in the presence of 1 or 2 wt% guaiacol in the feed, the net rate of consumption of guaiacol in reactions with the lignin-derived fragments is higher than the net rate of formation of guaiacol from lignin depolymerisation. Strangely enough, at a low loading of guaiacol (0.2 wt%), the guaiacol was formed at a slightly higher rate than it was consumed: the final content of guaiacol was 114 % of the amount added, see Figure S1B. It is interesting to note that the fraction of guaiacol remaining after the reaction was lower when lignin was added, see Figure S1B. Although the exact reactions are unknown, it is likely that there are several reaction paths, particularly for the consumption of guaiacol because it can react with different lignin fragments. It is possible that lignin increases the consumption of guaiacol by reacting with it.

The high M_w products from guaiacol polymerisation are not observed in the samples with lignin, see Figure S2. This indicates that guaiacol reacts faster with fragments generated by depolymerisation of lignin than with itself, else there should be traces of guaiacol oligomers in the molecular weight distributions of the ASO fractions with lignin added. An alternative possibility is that the higher pH when guaiacol is run without lignin, seen in the higher product phase pH in Table 1, could promote polymerisation of guaiacol.

3.2 Yields of product fractions

The yields of the three product fractions char, PS and ASO versus the dry lignin loaded are presented in Figure 3. The dominating product fraction is clearly the PS. It is likely that most of the non-reacted guaiacol ended up in the ASO fraction, since guaiacol is soluble in the reaction mixture; the yields for this fraction are presented with this guaiacol included.

The amount of char formed increases with increasing guaiacol charge and residence time, see Figure 3. The filter cake forming the char was washed with water and only showed minor amounts of guaiacol in the molecular weight distribution, see Figure S3. This indicates that the increase in yield of char when guaiacol is added is an effect of guaiacol promoting char formation, rather than non-reacted residual guaiacol ending up in the char phase.

In Figure 3A it can be seen that, at a short residence time of 1 min, the addition of 2 wt% guaiacol in the reaction mixture results in a char yield of 12 % ± 4 %, which should be compared to a yield of 0 % when no guaiacol was added. Guaiacol thus reacts rapidly (within 1 min) with the
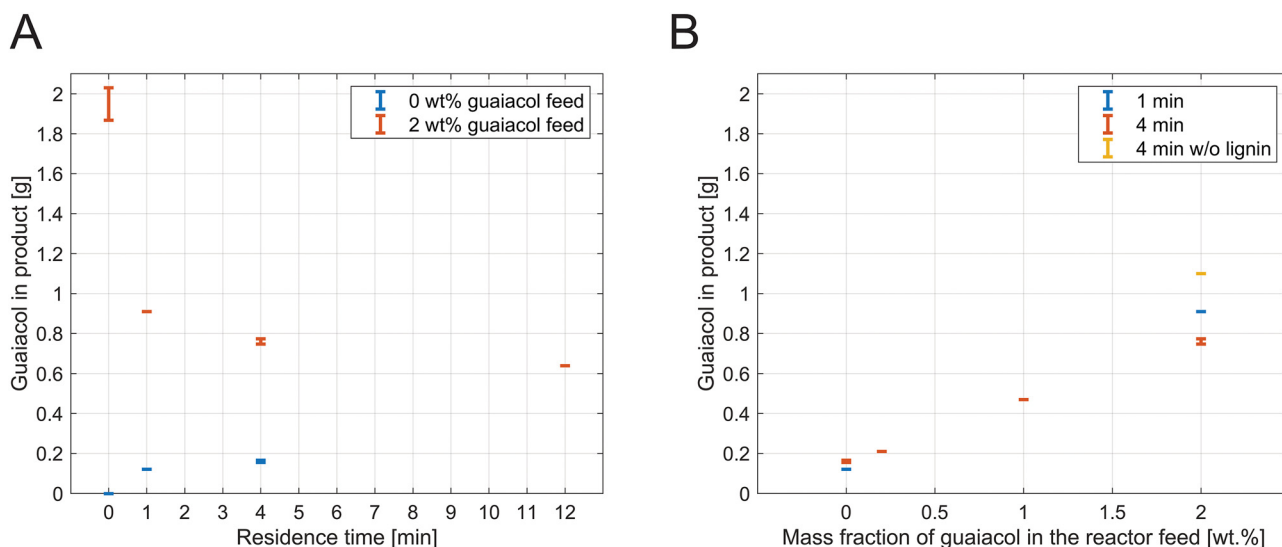
Figure 2: Mass of guaiacol in the reaction mixture versus residence time (A) and mass fraction of guaiacol in the reactor feed (B) at average reactor temperatures and pressures of 288–301 °C and 214–251 bar, respectively. Data for 0 min of residence time in (A) is the average amount of guaiacol injected into the reactor.
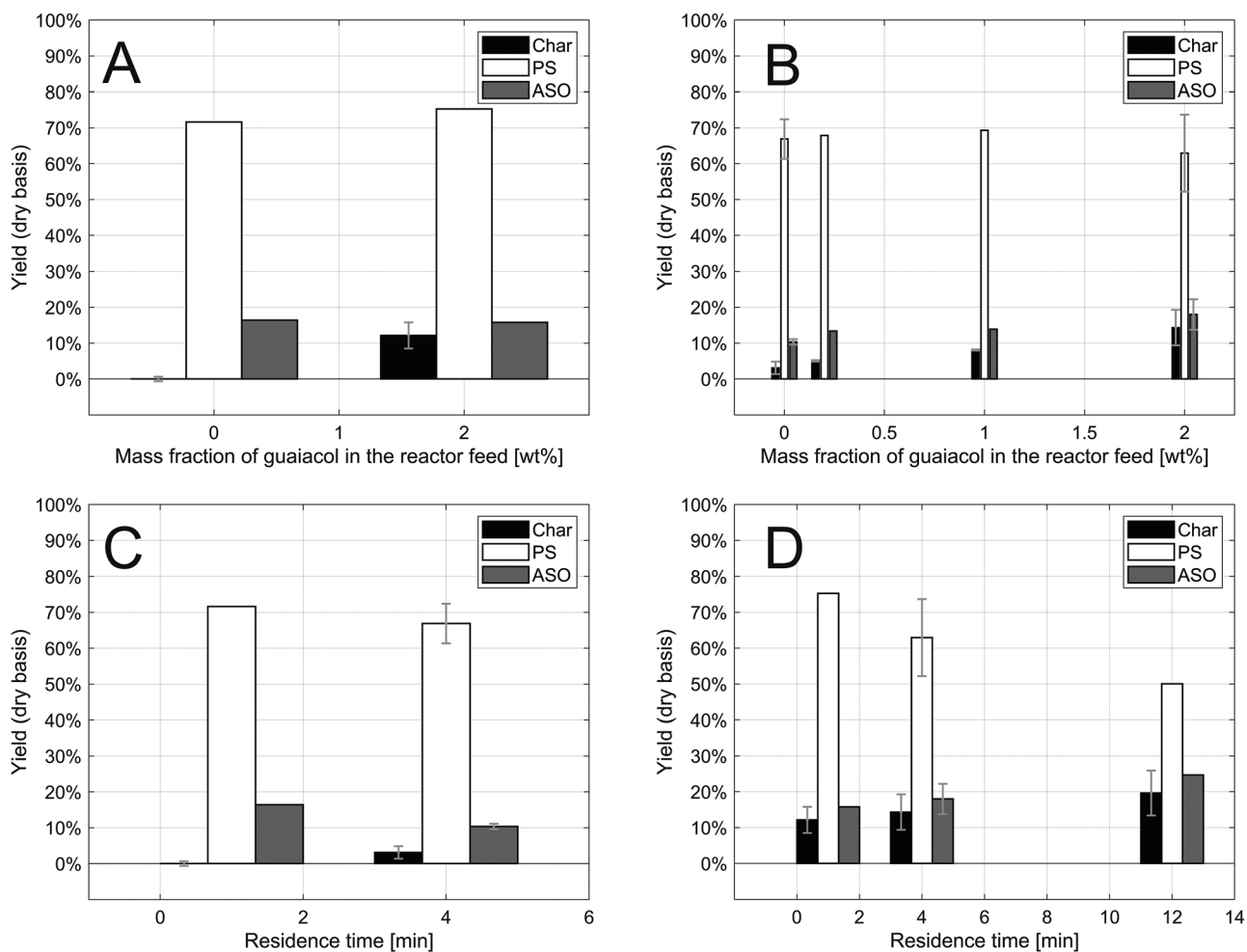

Figure 3: Yields of product fractions run at average reactor temperatures and pressures of 288–301 °C and 214–251 bar at varying mass fractions of guaiacol in the feed at 1 min (A) and 4 min (B) residence times, respectively, and at varying residence times with 0 wt% (C) and 2 wt% (D) guaiacol in the feed, respectively.

depolymerised lignin molecules and forms new molecules that, to some extent, end up in the char; since they precipitate, it is likely that these new molecules are non-polar (Ahlbom et al. 2022). At a longer residence time of 4 min, char is formed without any guaiacol in the feed, see Figure 3B and C. Consequently, while the reaction conditions are thus sufficiently harsh to yield char at 4 min without guaiacol, adding guaiacol causes its formation to occur sooner, at 1 min already. On the other hand, the PS fraction is largely unaffected by the guaiacol addition, see Figure 3A and B, but the yield decreases with increasing residence time, see Figure 3C and D. The yield of the ASO fraction is seen to increase somewhat with increased guaiacol feed and residence times with guaiacol added, see Figure 3B and D.

3.3 Molecular weights

The weight average molecular weights, M_w, of the product fractions and the original lignin are presented in Tables 2 and 3. It is clear that hydrothermal treatment reduces the M_w of the products (char, PS and ASO fractions) compared to the original lignin. The PS fraction has the highest M_w, the char fraction shows a lower M_w and the ASO exhibits the lowest M_w. The molecular weight distributions from which the M_w in Table 2 are calculated are given in Figures 4 and S4.

Table 2 reports the M_w of the product fractions at 1 and 4 min of residence time. It is obvious that increasing the guaiacol feed from 0 to 2 wt% decreases the M_w of the char at 4 min and of PS fractions at both 1 and 4 min of residence time.

Guaiacol had the strongest influence on the M_w of the char fraction, in which it decreased as the addition of guaiacol increased. The M_w of the PS, on the other hand,

Table 2: Weight average molecular weight (M_w) of the original lignin and the products fractions, with standard deviations for duplicate reactor runs at 1 and 4 min of residence time, respectively.

Mass fraction of guaiacol in the feed [wt%]	M_w Char [kDa]	M_w PS [kDa]	M_w ASO [kDa]
LignoBoost lignin			11.8 ± 0.1
1 min residence time			
0	–	7.9	1.3
2	3.6	5.5	1.5
4 min residence time			
0	7.0 ± 0.4	7.8 ± 0.2	1.5 ± 0.1
0.2	6.5	6.3	1.4
1	4.2	6.1	1.5
2	3.7 ± 0.4	6.3 ± 0.2	2.1 ± 0.1

No char was formed at 0 wt% guaiacol in the feed at 1 min of residence time.

Table 3: Weight average molecular weight (M_w) of the original lignin and the product fractions, with standard deviations, at 0 and 2 wt% guaiacol in the feed, respectively.

Residence time [min]	M_w Char [kDa]	M_w PS [kDa]	M_w ASO [kDa]
LignoBoost lignin			11.8 ± 0.1
0 wt% guaiacol in the feed			
1	–	7.9	1.3
4	7.0 ± 0.4	7.8 ± 0.2	1.5 ± 0.1
2 wt% guaiacol in the feed			
1	3.6	5.5	1.5
4	3.7 ± 0.4	6.3 ± 0.2	2.1 ± 0.1
12	4.7	6.6	2.0

No char was formed at 1 min of residence time with 0 wt% guaiacol in the feed.

seemed to be affected when some guaiacol, 0.2 wt%, was added but further additions in the range 0.2–2 wt% did not have any significant effect. This could also be found in the molecular weight distributions presented in Figures 4A and S4A: it is from these distributions the M_w in Table 2 are calculated. More pronounced shifts in the molecular weight distributions with higher guaiacol feeds are seen in the char fraction, see Figure 4A1, than for the PS and ASO fractions, see Figure 4A2 and A3, respectively. This is in accordance with the greater change in M_w of the char fraction compared to the PS and ASO fractions. Adding 0.2 wt% guaiacol to the reaction mixture does not change the molecular weight distribution of the char fraction as much as in the PS fraction. Instead, increasing the amount of guaiacol is necessary, from 0.2 to 1 wt% guaiacol, to change the char molecular weight distribution significantly, see Figure 4A1.

In Figure 4A it can also be found that, for both the char and the PS fractions, the content of high-molecular weight material decreases, and the content of low-molecular weight material increases with increasing guaiacol charge, thereby showing the capping effect of guaiacol. For the ASO fraction, it seems that the content of high molecular weight material increases slightly with increasing guaiacol charge, see Figure 4A3: this may be due to the fact that guaiacol reacts with some low molecular weight compounds of lignin, forming structures with a higher molecular weight.

The M_w of the product fractions at different residence times with 0 and 2 wt% added guaiacol are shown in Table 3. Here, it can be seen that, after initial depolymerisation of the lignin within the first minute, the M_w increases with increasing residence time as the products show a net repolymerisation, which begins at different times for the various product fractions. Figure 4B and S4B present the
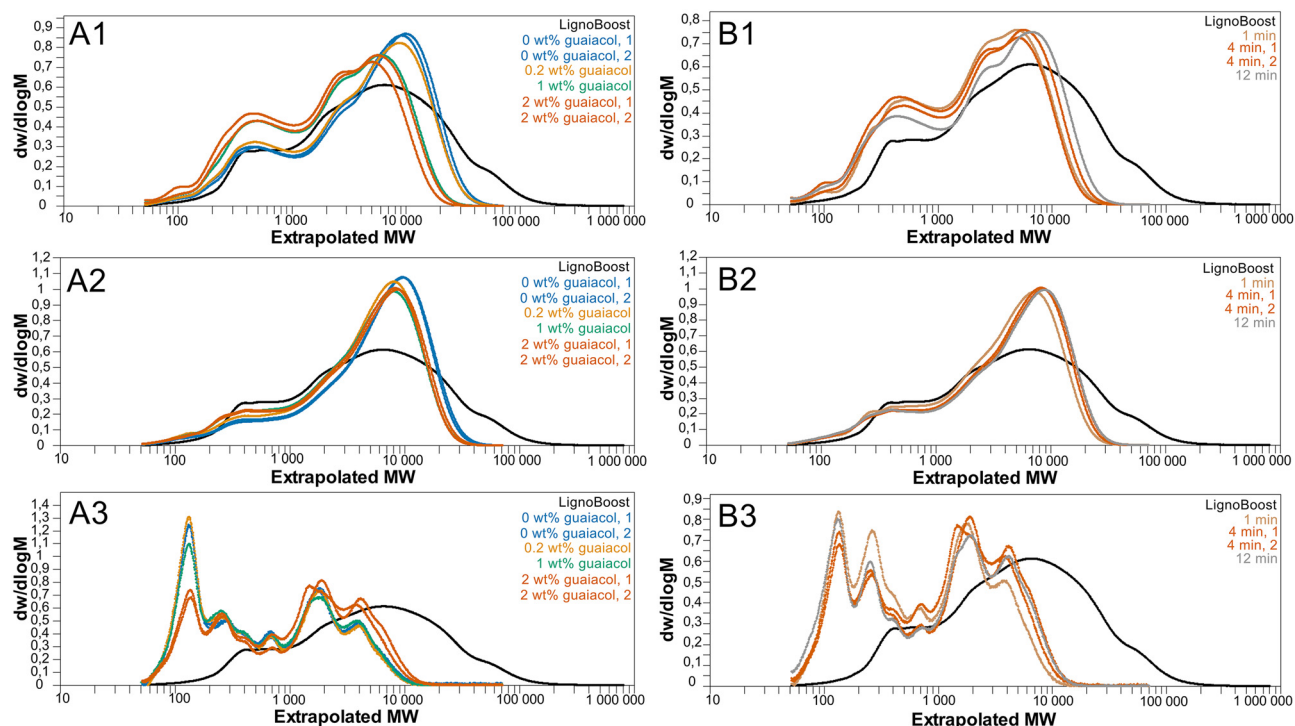
Figure 4: Molecular weight distributions of the char (1), PS (2) and ASO (3) fractions at 4 min residence time and varying mass fractions of guaiacol in the feed (A), and with 2 wt% guaiacol in the feed at different residence times (B). The unit is Da.

molecular weight distributions from which the M_w in Table 3 is calculated. For the char fraction in particular, it is obvious that the repolymerisation that occurs with increasing residence time results in shifts to the right, to higher molecular weights, see Figure 4B1. The same is seen for the PS and ASO fractions, but to a lesser degree. This indicates that a fast initial depolymerisation is followed by reaction steps where product molecules, oligomers and polymers react further, forming larger molecules and even polymers. These reactions are nevertheless slower than the initial depolymerisation. Thus, in order to minimise the molecular weight of the products, the residence time should be short and at least some guaiacol should be added.

3.4 Changes in molecular structure

The inter-unit region of the NMR spectrum shows cleavage of the inter-unit ether linkages in both the char and the PS fractions, see Figure S5. 1 min of residence time in the reactor causes the peaks of the inter-unit ether linkages, β-O-4′, β-β′ and β-5′, to disappear, i.e. these inter-unit ether linkages are lost in the char and PS fractions, as shown in previous work by Ahlbom et al. (2022). The breaking of the inter-unit ether

linkages was also found at the longer residence times of 4 and 12 min, as well as without guaiacol. It thus seems that the hydrothermal conditions in themselves cleave the inter-unit ether linkages rapidly, regardless of whether guaiacol is added or not. The original lignin depolymerises, which agrees not only with the reduction in M_w given in Tables 2 and 3 but also the loss in high molecular weight compounds shown in Figure 4B.

Signals for residual guaiacol should show up in the aromatic region (Giummarella et al. 2020). These signals are located under the aromatic peaks for the char and PS fraction and therefore hard to distinguish. In Figure 5 the aromatic regions of the lignin (A), the PS fraction at 1 min of residence time without guaiacol in the feed (B) and with 2 wt% guaiacol in the feed (C), are presented. With the addition of guaiacol, new peaks emerge in the PS fraction, see Figure 5C. The peaks that emerge are highlighted with a black oval; the very same peaks also appear in the aromatic region of the char spectra when guaiacol is added after 4 min of reaction, see Figure S6. The intensity of these new peaks also increases at longer residence times for both char and PS. Giummarella et al. (2020) obtained similar peaks in HSQC spectrum for guaiacol oligomers polymerised, by radical coupling, with hydrogen peroxide and horseradish
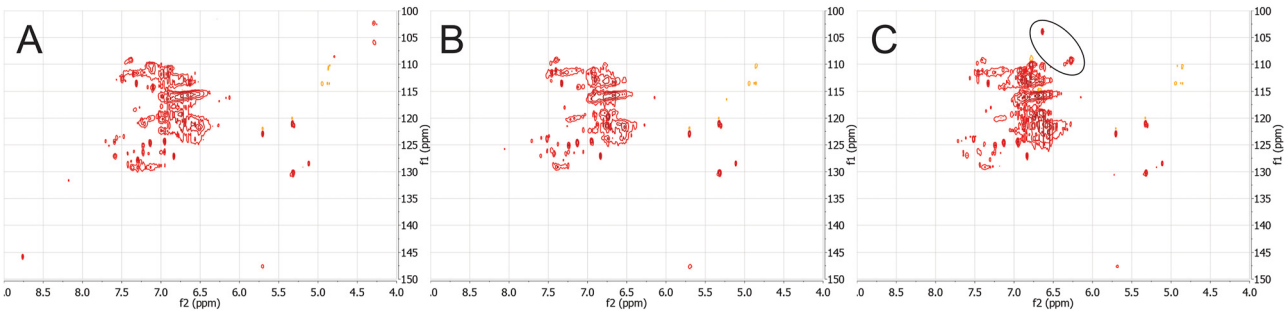
Figure 5: Aromatic region of the HSQC spectrum of lignin (A), the PS fraction run at 1 min of residence time without guaiacol in the feed (B) and with 2 wt% guaiacol in the feed (C). N.B. The new peaks that emerge when guaiacol is added are circled in black.

peroxidase. Thus, while these new peaks could be the result of guaiacol reacting with lignin fragments, they could also be traces of the polymerisation of guaiacol, similar to the polymerisation of guaiacol in the control sample, see Figure S2. Potentially, the guaiacol could be coupled in a radical reaction in this case too, just as in the work by Giummarella et al. (2020).

3.5 Yields of monoaromatic compounds

Monoaromatic compounds in the ASO fractions were identified, and semi-quantified, by GC-MS. Most were found to be guaiacol derivatives, even when guaiacol was not added to the reaction mixture. Since the lignin is sourced from softwood, and thus comprised of guaiacyl propane units, this is in line with expectations. Control measurements made on the diethyl ether extract of dissolved, unreacted lignin showed no monoaromatic compounds, suggesting that hydrothermal treatment is indeed required if the depolymerisation of lignin is to form monoaromatic components.

Table 4 reports the yields of monoaromatic components versus dry lignin at 1 and 4 min of residence time. Guaiacol is excluded because it dominates the monoaromatic compounds identified, even when it is not added to the feed. With increasing amounts of guaiacol added, the yields of monoaromatic compounds identified by GC-MS increase. For instance, the yield of 1,2-dimethoxybenzene, earlier mentioned as a product of guaiacol reacting without lignin, increases with the addition of guaiacol to the reaction mixture.

Figure 6 shows the yields of monoaromatic components with 0 wt% guaiacol addition for 1 and 4 min of residence time. These yields increase with residence time, with the exception of vanillin. Guaiacol was also identified by GC-MS: with a yield of 2–2.5 % on dry lignin, it dominated the yield of monoaromatic components and is therefore not given in

Table 4: Yields of monoaromatic components identified and semi-quantified by GC-MS versus dry lignin, without guaiacol and at 1 and 4 min of residence time, respectively.

Mass fraction of guaiacol in the feed [wt%]	Yield of monoaromatic components, excluding guaiacol [%]
1 min residence time	
0	0.4
2	1.7 ± 0.7
4 min residence time	
0	0.5 ± 0.0
0.2	0.9
1	2.0
2	2.9 ± 0.7

An average value, with corresponding standard deviation, is given for samples with duplicate reactor runs.

Figure 6. The yield of guaiacol versus dry lignin increased with residence time at 0 wt% guaiacol in the feed, thereby agreeing with the result shown in Figure 2A.

Figure 7 shows the yields of monoaromatic components obtained at different residence times with the addition of 2 wt% guaiacol. Since guaiacol was added to the feed, the product is dominated by guaiacol and it is therefore excluded. However, like in Figure 2A, the guaiacol yield level, semi-quantified with GC-MS, was seen to drop with increasing residence time. It is notable that the yields of monoaromatic compounds are higher with guaiacol added to the feed than without the addition of guaiacol, cf. Figures 6 and 7. Catechol was not separated reliably from 4-methyl guaiacol; at 12 min of residence time, the catechol value therefore contains an unknown fraction of 4-methyl guaiacol. With increasing residence time, the 1,2-dimethoxybenzene, 4-methyl guaiacol and catechol appear to increase somewhat with time, although they remain at low levels. It could be hypothesised that alkyl guaiacols form either from the
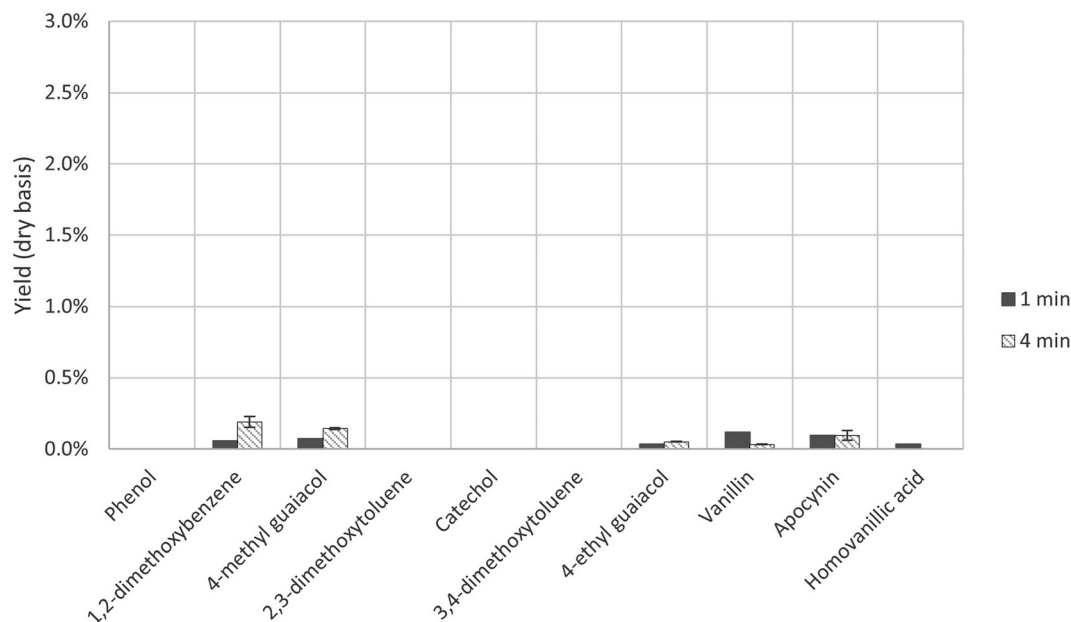
Figure 6: Yields of monoaromatic compounds identified and semi-quantified by GC-MS, with standard deviations for duplicate reactor runs, versus dry lignin at 0 wt% guaiacol feed at different residence times. The yield of guaiacol is excluded.
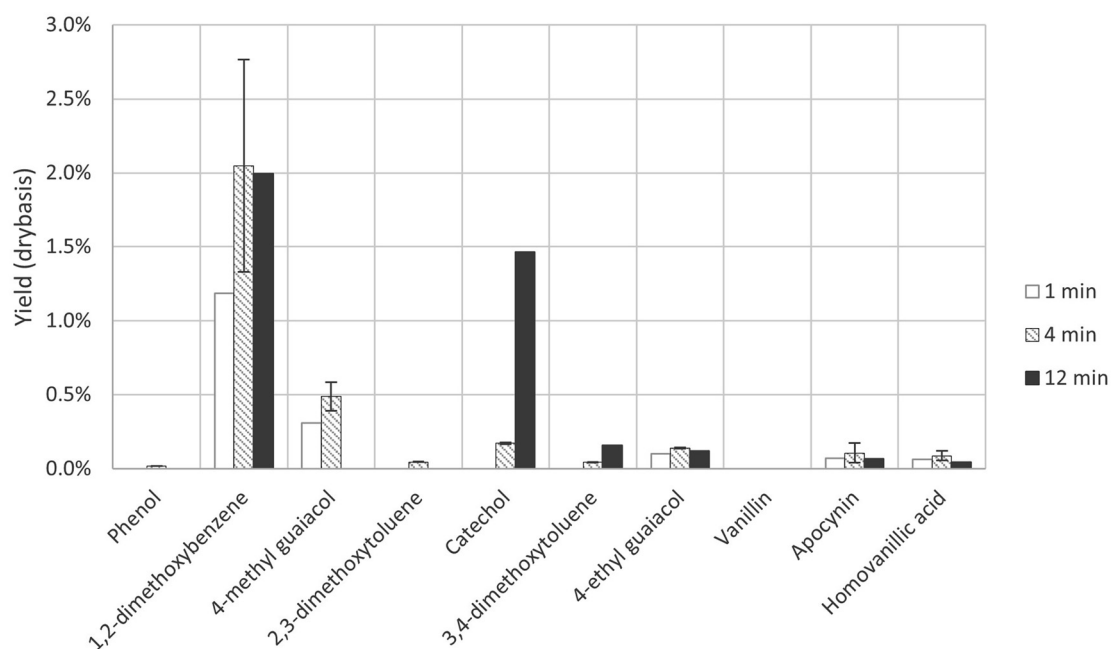

Figure 7: Yields of monoaromatic compounds identified and semi-quantified by GC-MS, with standard deviations for duplicate reactor runs, versus dry lignin at 2 wt% guaiacol feed for different residence times. N.B. The yield of catechol could include an unknown amount of 4-methyl guaiacol. The yield of guaiacol is excluded.

depolymerisation of lignin or alkylation of the guaiacol, in a fashion similar to that observed in previous works in which phenol was used as a capping agent (Arturi et al. 2017; Barbier et al. 2012; Saisu et al. 2003). The loss of guaiacol is nevertheless greater than the gain of alkyl guaiacols, which can be explained at least partly by the polymerisation of guaiacol.

4 Discussion

The yield of char increases with increasing additions of guaiacol, see Figure 3A and B, although the M_w of this fraction decreases simultaneously, see Table 2. The addition of guaiacol thus affects the reactions and repolymerisation of the reactive lignin fragments, promoting the production of lower molecular weight compounds. The net effect of adding guaiacol is nonetheless an increase in the production of char.

At 2 wt% added guaiacol, net repolymerisation of the precipitated solids (PS) fractions began to be noticeable already at residence times longer than 1 min, see Table 3, whereas net repolymerisation of char occurred between 4 and 12 min. The repolymerisation of the reaction products was also noted in similar lignin depolymerisation experiments that did not have NaOH in the reaction mixture and used isopropanol as a capping agent (Ahlbom et al. 2022): repolymerisation began to be noticeable between 4 and 12 min after an initial depolymerisation, which is very similar to the char fraction in the present study.

Increasing the residence time appears to cause an increase in the yield of char. This is also analogous to previous work using isopropanol as a capping agent, where increasing residence times caused an increase in the yield of char coupled with a decrease in that of PS. Rapid depolymerisation was also seen by NMR in that particular set-up (Ahlbom et al. 2022).

Interestingly enough, the results show that more guaiacol is formed than consumed when 0.2 wt% guaiacol was added to the reaction mixture: there is a net formation of guaiacol. At some level of guaiacol in the reaction mixture, its net consumption must nevertheless equal its net formation. Based on the data obtained in this study, the hypothesis could be proposed that the shift from net production to net consumption lies somewhere in between 0.2 and 1 wt% of guaiacol in the feed, see Figure S1. Using an addition of 0.2 wt% guaiacol, however, did not have an evident capping effect at 4 min of residence time comparing to the sample run without guaiacol: the M_w of the char did not decrease significantly, and its yield increased.

5 Conclusions

Kraft lignin was depolymerised in alkaline reaction conditions at 290 °C and 250 bar, with guaiacol added as a capping agent. At these conditions, inter-unit ether linkages in the lignin were cleaved within 1 min of residence time.

Guaiacol is both a product and a reactant in the reaction system; the reaction kinetics appear to depend on the mass fraction of guaiacol in the feed. The guaiacol itself polymerises to a high molecular weight product, which remains soluble in the aqueous product phase. However, guaiacol appears to react more rapidly with added lignin than with itself: the residual content of guaiacol in the product is lower when lignin is added, and no soluble guaiacol polymer is found in the product.

The addition of guaiacol increases the yield of char, both at 1 and 4 min of residence time. The guaiacol does, however, cause the M_w of the char to be reduced; the M_w of the PS is also reduced.

Increasing the residence time in the reactor above 4 min causes a net repolymerisation, which is observed as an increase in the M_w of the char. Thus, in order to obtain lower M_w products, a short residence time and the addition of guaiacol are beneficial, although the latter comes with a higher char yield. The use of guaiacol as a capping agent might therefore not be ideal.

References

Abdelaziz, O.Y., Li, K., Tunå, P., and Hulteberg, C.P. (2018). Continuous catalytic depolymerisation and conversion of industrial kraft lignin into low-molecular-weight aromatics. Biomass Convers. Biorefinery 8: 455–470, https://doi.org/10.1007/s13399-017-0294-2.

Ahlbom, A., Maschietti, M., Nielsen, R., Hasani, M., and Theliander, H. (2022). Towards understanding kraft lignin depolymerisation under hydrothermal conditions. Holzforschung 76: 37–48, https://doi.org/10.1515/hf-2021-0121.

Ahlbom, A., Maschietti, M., Nielsen, R., Lyckeskog, H., Hasani, M., and Theliander, H. (2021). Using isopropanol as a capping agent in the hydrothermal liquefaction of kraft lignin in near-critical water. Energies 14: 932, https://doi.org/10.3390/en14040932.

Arturi, K.R., Strandgaard, M., Nielsen, R.P., Søgaard, E.G., and Maschietti, M. (2017). Hydrothermal liquefaction of lignin in near-critical water in a new batch reactor: influence of phenol and temperature. J. Supercrit. Fluids 123: 28–39, https://doi.org/10.1016/j.supflu.2016.12.015.

Balakshin, M.Y., Capanema, E.A., Sulaeva, I., Schlee, P., Huang, Z., Feng, M., Borghei, M., Rojas, O.J., Potthast, A., and Rosenau, T. (2021). New opportunities in the valorization of technical lignins. ChemSusChem 14: 1016–1036, https://doi.org/10.1002/cssc.202002553.

Barbier, J., Charon, N., Dupassieux, N., Loppinet-Serani, A., Mahé, L., Ponthus, J., Courtiade, M., Ducrozet, A., Quoineaud, A.-A., and Cansell, F. (2012). Hydrothermal conversion of lignin compounds. A detailed study of fragmentation and condensation reaction pathways. Biomass Bioenergy 46: 479–491, https://doi.org/10.1016/j.biombioe.2012.07.011.

Belkheiri, T., Andersson, S.-I., Mattsson, C., Olausson, L., Theliander, H., and Vamling, L. (2018). Hydrothermal liquefaction of kraft lignin in subcritical water: influence of phenol as capping agent. Energy Fuels 32: 5923–5932, https://doi.org/10.1021/acs.energyfuels.8b00068.

Belkheiri, T., Vamling, L., Nguyen, T.D.H., Maschietti, M., Olausson, L., Andersson, S.-I., Åmand, L.-E., and Theliander, H. (2014). Kraft lignin depolymerization in near-critical water: effect of changing co-solvent. Cellul. Chem. Technol. 48: 813–818.

Brand, S., Hardi, F., Kim, J., and Suh, D.J. (2014). Effect of heating rate on biomass liquefaction: differences between subcritical water and supercritical ethanol. Energy 68: 420–427, https://doi.org/10.1016/j.energy.2014.02.086.

Cao, Y., Zhang, C., Tsang, D.C.W., Fan, J., Clark, J.H., and Zhang, S. (2020). Hydrothermal liquefaction of lignin to aromatic chemicals: impact of lignin structure. Ind. Eng. Chem. Res. 59: 16957–16969, https://doi.org/10.1021/acs.iecr.0c01617.

Cheng, S., Wilks, C., Yuan, Z., Leitch, M., and Xu, C. (Charles) (2012). Hydrothermal degradation of alkali lignin to bio-phenolic compounds in sub/supercritical ethanol and water-ethanol co-solvent. Polym. Degrad. Stab. 97: 839–848, https://doi.org/10.1016/j.polymdegradstab.2012.03.044.

Crestini, C., Lange, H., Sette, M., and Argyropoulos, D.S. (2017). On the structure of softwood kraft lignin. Green Chem. 19: 4104–4121, https://doi.org/10.1039/c7gc01812f.

Dessbesell, L., Paleologou, M., Leitch, M., Pulkki, R., and Xu, C. (Charles) (2020). Global lignin supply overview and kraft lignin potential as an alternative for petroleum-based polymers. Renew. Sustain. Energy Rev. 123: 109768, https://doi.org/10.1016/j.rser.2020.109768.

Galkin, M.V. and Samec, J.S.M. (2016). Lignin valorization through catalytic lignocellulose fractionation: a fundamental platform for the future biorefinery. ChemSusChem 9: 1544–1558, https://doi.org/10.1002/cssc.201600237.

Gellerstedt, G. (2015). Softwood kraft lignin: raw material for the future. Ind. Crops Prod. 77: 845–854, https://doi.org/10.1016/j.indcrop.2015.09.040.

Giummarella, N., Lindén, P.A., Areskogh, D., and Lawoko, M. (2020). Fractional profiling of kraft lignin structure: unravelling insights on lignin reaction mechanisms. ACS Sustain. Chem. Eng. 8: 1112–1120, https://doi.org/10.1021/acssuschemeng.9b06027.

Goldmann, W.M., Anthonykutty, J.M., Ahola, J., Komulainen, S., Hiltunen, S., Kantola, A.M., Telkki, V.V., and Tanskanen, J. (2020). Effect of process variables on the solvolysis depolymerization of pine kraft lignin. Waste Biomass Valorization 11: 3195–3206, https://doi.org/10.1007/s12649-019-00701-1.

Guo, M., Maltari, R., Zhang, R., Kontro, J., Ma, E., and Repo, T. (2021). Hydrothermal depolymerization of kraft lignins with green C1-C3 alcohol-water mixtures. Energy Fuel. 35: 15770–15777, https://doi.org/10.1021/acs.energyfuels.1c01968.

Hernández-Ramos, F., Fernández-Rodríguez, J., Alriols, M.G., Labidi, J., and Erdocia, X. (2020). Study of a renewable capping agent addition in lignin base catalyzed depolymerization process. Fuel 280: 118524, https://doi.org/10.1016/j.fuel.2020.118524.

Islam, M.N., Taki, G., Rana, M., and Park, J.H. (2018). Yield of phenolic monomers from lignin hydrothermolysis in subcritical water system. Ind. Eng. Chem. Res. 57: 4779–4784, https://doi.org/10.1021/acs.iecr.7b05062.

Jensen, M.M., Madsen, R.B., Becker, J., Iversen, B.B., and Glasius, M. (2017). Products of hydrothermal treatment of lignin and the importance of ortho-directed repolymerization reactions. J. Anal. Appl. Pyrolysis 126: 371–379, https://doi.org/10.1016/j.jaap.2017.05.009.

Kleinert, M. and Barth, T. (2008). Phenols from lignin. Chem. Eng. Technol. 31: 736–745, https://doi.org/10.1002/ceat.200800073.

Kruse, A. and Dahmen, N. (2015). Water – a magic solvent for biomass conversion. J. Supercrit. Fluids 96: 36–45, https://doi.org/10.1016/j.supflu.2014.09.038.

Lappalainen, J., Baudouin, D., Hornung, U., Schuler, J., Melin, K., Bjelić, S., Vogel, F., Konttinen, J., and Joronen, T. (2020). Sub- and supercritical water liquefaction of kraft lignin and black liquor derived lignin. Energies 13: 3309, https://doi.org/10.3390/en13133309.

Lawson, J.R. and Klein, M.T. (1985). Influence of water on guaiacol pyrolysis. Ind. Eng. Chem. Fundam. 24: 203–208, https://doi.org/10.1021/i100018a012.

Lee, H.-S., Jae, J., Ha, J.-M., and Suh, D.J. (2016). Hydro- and solvothermolysis of kraft lignin for maximizing production of monomeric aromatic chemicals. Bioresour. Technol. 203: 142–149, https://doi.org/10.1016/j.biortech.2015.12.022.

Mattsson, C., Andersson, S.I., Belkheiri, T., Åmand, L.E., Olausson, L., Vamling, L., and Theliander, H. (2016). Using 2D NMR to characterize the structure of the low and high molecular weight fractions of bio-oil obtained from LignoBoost™ kraft lignin depolymerized in subcritical water. Biomass Bioenergy 95: 364–377, https://doi.org/10.1016/j.biombioe.2016.09.004.

Nguyen, T.D.H., Maschietti, M., Belkheiri, T., Åmand, L.E., Theliander, H., Vamling, L., Olausson, L., and Andersson, S.I. (2014). Catalytic depolymerisation and conversion of Kraft lignin into liquid products using near-critical water. J. Supercrit. Fluids 86: 67–75, https://doi.org/10.1016/j.supflu.2013.11.022.

Okuda, K., Umetsu, M., Takami, S., and Adschiri, T. (2004). Disassembly of lignin and chemical recovery – rapid depolymerization of lignin without char formation in water-phenol mixtures. Fuel Process. Technol. 85: 803–813, https://doi.org/10.1016/j.fuproc.2003.11.027.

Roberts, V.M., Stein, V., Reiner, T., Lemonidou, A., Li, X., and Lercher, J.A. (2011). Towards quantitative catalytic lignin depolymerization. Chem. – A Eur. J. 17: 5939–5948, https://doi.org/10.1002/chem.201002438.

Saisu, M., Sato, T., Watanabe, M., Adschiri, T., and Arai, K. (2003). Conversion of lignin with supercritical water-phenol mixtures. Energy Fuels 17: 922–928, https://doi.org/10.1021/ef0202844.

Taurog, A., Dorris, M.L., and Guziec, F.S. (1992). An unexpected side reaction in the guaiacol assay for peroxidase. Anal. Biochem. 205: 271–277, https://doi.org/10.1016/0003-2697(92)90434-9.

Toledano, A., Serrano, L., and Labidi, J. (2014). Improving base catalyzed lignin depolymerization by avoiding lignin repolymerization. Fuel 116: 617–624, https://doi.org/10.1016/j.fuel.2013.08.071.

Toor, S.S., Rosendahl, L., and Rudolf, A. (2011). Hydrothermal liquefaction of biomass: a review of subcritical water technologies. Energy 36: 2328–2342, https://doi.org/10.1016/j.energy.2011.03.013.

Wahyudiono, Kanetake, T., Sasaki, M., and Goto, M. (2007). Decomposition of a lignin model compound under hydrothermal conditions. Chem. Eng. Technol. 30: 1113–1122, https://doi.org/10.1002/ceat.200700066.

Wahyudiono, Sasaki, M., and Goto, M. (2011). Thermal decomposition of guaiacol in sub- and supercritical water and its kinetic analysis. J. Mater. Cycles Waste Manag. 13: 68–79, https://doi.org/10.1007/s10163-010-0309-6.